haematologica
Journal of the Ferrata Storti Foundation

Real-world minimal residual disease assessment in multiple myeloma using a standardized flow cytometry approach: feasibility, clinical implications, and immune correlates from a single-center experience

by Cirino Botta, Andrea Rizzuto, Maria Speciale, Emilia Gigliotta, Anna Maria Corsale, Francesco Romano, Irene Mussotto, Cristina Aquilina, Andrea Romano, Marta Biondo, Elena Tofacchi, Marta Di Simone, Miriam Sciortino, Fulvio Brucato, Gianluca Guercio, Miriam Di Caro, Anxur Merenda, Stefania Vasta, Concetta Scazzone, Giulia Bivona, Valentina Calò, Marco Pio La Manna, Nadia Caccamo, Francesco Dieli, Sergio Siragusa and Serena Meraviglia

Received: March 12, 2026.
Accepted: August 21, 2026.

Citation: Cirino Botta, Andrea Rizzuto, Maria Speciale, Emilia Gigliotta, Anna Maria Corsale, Francesco Romano, Irene Mussotto, Cristina Aquilina, Andrea Romano, Marta Biondo, Elena Tofacchi, Marta Di Simone, Miriam Sciortino, Fulvio Brucato, Gianluca Guercio, Miriam Di Caro, Anxur Merenda, Stefania Vasta, Concetta Scazzone, Giulia Bivona, Valentina Calò, Marco Pio La Manna, Nadia Caccamo, Francesco Dieli, Sergio Siragusa and Serena Meraviglia. Real-world minimal residual disease assessment in multiple myeloma using a standardized flow cytometry approach: feasibility, clinical implications, and immune correlates from a single-center experience.
Haematologica. 2026 Sept 3. doi: 10.3324/haematol.2026.300864 [Epub ahead of print]

Real-world minimal residual disease assessment in multiple myeloma using a standardized flow cytometry approach: feasibility, clinical implications, and immune correlates from a single-center experience

Cirino Botta[1], Andrea Rizzuto[1], Maria Speciale[1,2], Emilia Gigliotta[1], Anna Maria Corsale[1,3], Francesco Romano[4], Irene Mussotto[1], Cristina Aquilina[1], Andrea Romano[1,2], Marta Biondo[1], Elena Tofacchi[1], Marta Di Simone[1,3] , Miriam Sciortino[3], Fulvio Brucato[3], Gianluca Guercio[3], Miriam Di Caro[1,3], Anxur Merenda[5], Stefania Vasta[5], Concetta Scazzone[3], Giulia Bivona[3], Valentina Calò[3], Marco Pio La Manna[3], Nadia Caccamo[3], Francesco Dieli[3], Sergio Siragusa[1*] and Serena Meraviglia[3*]

[1] Department of Health Promotion, Mother and Child Care, Internal Medicine and Medical Specialties (ProMISE), University of Palermo, Palermo, Italy

[2] University of Palermo, Department of Surgical, Oncological and Stomatological Disciplines (DICHIRONS), Palermo, Italy;

[3] Central Laboratory of Advanced Diagnosis and Biomedical Research, University of Palermo, Palermo, Italy;

[4] Dana-Farber/Boston Children's Cancer and Blood Disorder Center, Harvard Medical School, Boston, MA, United States;

[5] UOSD Oncoematologia, ARNAS Ospedale Civico, Palermo, Italy;

[*]equally contributed to this work and should be considered as co-last authors

Correpondence to: Cirino Botta, cirino.botta@unipa.it

Running heads: **Real-world assessment of MRD in multiple myeloma**

Authors' Contributions: C.B. conceived the study, designed the experimental work, and is the corresponding author. C.B., S.S., and S.M. contributed to the conceptualization of the manuscript. C.B., A.Ri., M.Sp., E.G., A.M.C., F.R., I.M., C.A., A.Ro., M.B., E.T., and M.D.S. were responsible for data collection and analysis. M.Sc., F.B., G.G., and M.D.C. performed and curated flow cytometry experiments. A.Me., S.V., C.S., G.B., V.C., M.P.L.M., N.C., and F.D. contributed to manuscript writing and supervision. All authors reviewed and approved the final version of the manuscript.

Conflict of Interest: The authors declare no conflicts of interest.

Fundings: This work was supported by grants from the Italian Association for Cancer Research (AIRC) within the My First AIRC Grant 2020 (no. 24534, 2021/2025), Progetti di Rilevante Interesse Nazionale (PRIN) 2022 (no. 20229JM25N), PRIN National Recovery and Resilience Plan (PNRR) 2022 (P2022E2JSK)

Data Sharing Statement: The data that support the findings of this study are available from the corresponding author upon reasonable request, provided that the request is adequately justified and compliant with institutional and ethical regulations.

Abstract

Minimal residual disease (MRD) assessment has emerged as a key prognostic marker in multiple myeloma (MM), with MRD negativity (undetectable MRD, uMRD) correlating with improved progression-free and overall survival. The International Myeloma Working Group recommends standardized protocols for MRD detection, including the EuroFlow-based next-generation flow cytometry (NGF), although its implementation in routine care remains challenging. We evaluated the feasibility and clinical utility of two CE-IVD-approved EuroFlow tubes for MRD detection in a real-world clinical setting, and investigated the relationship between bone marrow (BM) immune profiles and disease outcomes. Between December 2021 and February 2024, 74 MM patients (58 of them classified as transplant-eligible) underwent 97 MRD evaluations after achieving at least a very good partial response (VGPR). Using ≥2 million events/sample, a median sensitivity of 10^{-5} was achieved; 45% of cases were uMRD. After a median follow-up of 19 months, one relapse occurred in the uMRD group, whereas 15 relapses and 3 deaths were observed among persistent MRD (pMRD) patients. Immunophenotypic profiling revealed a higher granulocyte-to-lymphocyte ratio and a lower proportion of $CD56^{dim}$ NK cells, possibly reflecting immune rebalancing after bone marrow recovery. Our findings confirm the feasibility and prognostic relevance of NGF-based MRD detection using standardized commercial panels, and highlight the potential of immune profiling to provide additional biological insights into MRD dynamics in multiple myeloma.

Introduction

Multiple myeloma (MM) is a heterogeneous hematologic malignancy characterized by the clonal proliferation of plasma cells in the bone marrow (BM), resulting in a range of clinical complications, including bone lesions, anemia, hypercalcemia, and renal dysfunction[1]. Over the past decade, the therapeutic landscape of MM has undergone a profound transformation, with the introduction of proteasome inhibitors, immunomodulatory drugs and monoclonal antibodies, significantly improving clinical outcomes[1]. Despite these advances, the disease remains largely incurable, with the majority of patients eventually experiencing relapse. This has underscored the need for more sensitive and clinically informative tools to monitor treatment response, guide therapeutic decisions, and improve long-term disease control. Among these, minimal residual disease (MRD) assessment has emerged as the most powerful prognostic tool currently available in MM[2]. MRD refers to the small number of residual malignant plasma cells that remain in the patient after treatment and are undetectable by conventional response criteria. The presence or absence of MRD after therapy has been shown to strongly correlate with progression-free survival (PFS) and overall survival (OS), across different treatment regimens, disease stages, and patient subgroups[2–5]. Recent meta-analyses and prospective studies have confirmed that MRD negativity, rather than complete response (CR) alone, is a more accurate predictor of long-term outcomes, making it a central endpoint in clinical trials and a potential marker for tailoring therapy in clinical practice[3,5]. In recognition of its prognostic significance, the International Myeloma Working Group (IMWG) has incorporated MRD evaluation into its response criteria and recommends its inclusion in the design of clinical trials. According to current IMWG guidelines, MRD assessment should be performed using standardized methods with a minimum sensitivity of 10^{-5}, meaning the assay must detect one malignant plasma cell among 100,000 bone marrow nucleated cells[6]. Two primary techniques are endorsed: next-generation flow cytometry (NGF) and next-generation sequencing (NGS)[2,6]. NGF, particularly the EuroFlow protocol, relies on highly standardized antibody panels and software tools to identify aberrant plasma cells with high specificity and sensitivity[7]. It allows for a comprehensive immunophenotypic characterization of BM cells and offers the advantage of a faster turnaround time. On the other hand, NGS techniques, such as the FDA-cleared ClonoSeq assay[8], detect clonal immunoglobulin gene rearrangements and can reach sensitivities as high as 10^{-6}, offering high precision and long-term clonotype tracking. While both NGF and NGS are highly sensitive and clinically validated, each presents distinct logistical and technical challenges. NGS requires baseline material, is relatively costly, and may have limited applicability in resource-constrained settings. NGF, although more accessible and versatile, remains underutilized outside of clinical trials, partly due to variability in instrumentation, antibody panels, and analytical expertise across laboratories. In routine clinical practice, MRD assessment is often performed using in-house adapted flow cytometry protocols, which may lack standardization and reproducibility. In particular, limited real-world data are available on the implementation of standardized CE-IVD NGF panels in routine clinical workflows, where logistical constraints, sample quality and heterogeneous treatment settings may affect assay performance.

An additional, emerging area of interest is the relationship between MRD status and the immunologic composition of the bone marrow microenvironment. There is growing evidence that treatment response and disease progression are influenced not only by the depth of tumor cell clearance but also by the degree and quality of immune reconstitution. Some studies have suggested that the persistence or recovery of specific immune subsets, such as T cells, NK cells, or myeloid populations, may correlate with MRD dynamics and patient outcomes[1,9–11]. However, these aspects are still rarely addressed in routine MRD assessments, largely because of the complexity of multiparametric flow cytometry datasets and the lack of standardized analytical frameworks that enable the simultaneous evaluation of residual tumor cells and the surrounding immune microenvironment. As a consequence, the relationship between MRD status and the broader immune landscape of the bone marrow remains insufficiently characterized, particularly in real-world clinical cohorts.. In this context, our study aimed to evaluate the feasibility and clinical relevance of MRD detection using two CE-IVD-approved EuroFlow-based flow cytometry panels—the Plasma Cell Screening Tube (PCST) and the Plasma Cell Disorders (PCD) tube—in a real-world, single-center cohort of patients with MM. In addition, we integrated immune profiling into the MRD assessment process by applying a semi-supervised computational workflow (FlowCT) for the unsupervised analysis of multiparametric flow cytometry data[12]. This approach allowed the simultaneous evaluation of MRD status and the characterization of the bone marrow immune microenvironment from the same datasets. Accordingly, the objectives of this study were twofold: (1) to assess the performance and implementation of a standardized NGF-based approach for MRD evaluation in a real-world clinical setting; and (2) to characterize the bone marrow immune landscape in patients within uMRD and pMRD, in order to explore potential immunologic correlates of treatment response.

Methods

Patients

This study was conducted as part of the prospective/retrospective study "MMVision," approved by the ethical committee of the Palermo University Hospital, reference numbers 02/2022 (codename: MMVision) and written informed consent was obtained from all participants in accordance with institutional guidelines and the Declaration of Helsinki. The assessment of MRD was carried out on BM samples from patients undergoing any treatment for MM when at least a very good partial response (VGPR) was achieved, considering the potential interference of Daratumumab. For patients eligible for ASCT, initial MRD evaluations included post-induction and 100 days post-ASCT. Subsequent MRD assessments were scheduled annually, in accordance with International Myeloma Working Group (IMWG) recommendations for "sustained uMRD”[6]. Baseline demographic and clinical data, collected from medical records, were included in the analysis. The variables considered in the analysis encompassed: age, sex, date of diagnosis, M-protein isotype, ISS stage, therapy, treatment cycle at the time of MRD evaluation and median PFS.

MRD assessment and quality check

BM samples from the initial pull, with an average volume ranging between 1–2 mL, were collected for each patient. Samples were stained using two CE-IVD EuroFlow-designed 8-color panels (PCST and PCD) from Beckton Dickinson. Both panels included the backbone markers CD45, CD138, CD38, and CD19 and four variable markers (CD56, ββ2-microglobulin, intracytoplasmic κ and λ light chains for PCST and CD28, CD27, CD117, and CD81 for PCD panel). The collected samples were processed as soon as possible after collection, typically on the same day or the following day, and always within 48 hours. Following collection, bone marrow samples were stored and transported at room temperature until processing. Sample quality was assessed throughout the analytical workflow. Samples showing evident clot formation were considered unsuitable for processing. During sample preparation, a viability dye was added and viable nucleated cells were counted by microscopy to estimate the amount of sample required for staining. Cell viability was routinely assessed as part of the quality control procedure, and no samples were excluded because of inadequate viability. Based on sample cellularity, the amount of marrow blood to be stained was estimated to achieve at least a 1×10^-5 limit of detection (LOD); therefore, the goal was to obtain at least 1 million events per tube, totaling at least 2 million events per MRD evaluation. Following acquisition, data quality was further assessed, including evaluation of potential hemodilution[13] and achievement of the minimum number of events required for MRD analysis. Samples not meeting predefined quality criteria were considered non-evaluable. To evaluate the potential impact of delayed processing on marker stability, samples processed within 24 hours from collection were compared with those processed between 24 and 48 hours after collection. Because plasma cells may be absent in MRD-negative samples and their immunophenotypic profile can vary substantially among patients, lymphocyte populations were selected as an internal biological control. The median fluorescence intensity (MFI) of all markers included in the EuroFlow PCD and PCST panels was assessed on lymphocyte subsets and compared according to processing time. All samples were acquired in a FACSLyric instrument (Beckton Dickinson) and data from both tubes of each patient were analyzed using Infinicyt Software (v.2.0.6; Cytognos/Beckton Dickinson).

Statistical Analysis

Kaplan-Meier curves were used to analyse the association between MRD status and PFS. Continuous data are shown as mean ± standard deviation or median. Categorical variables are presented as numbers or percentages. Differences between the two groups were assessed using the Student's t-test, chi-square test, or Mann–Whitney U test. Two-tailed statistical analysis was used, and p-values of <0.05 were considered statistically significant. R statistical software was used to analyse and represent clinical results (sankey plot, Kaplan meier curves, dot plots, swimmer plots) through, among others, the *ggpubr, ggplot2* and *survminer* packages.

BM immune-populations analysis

A comparative exploratory post-hoc analysis of the BM microenvironment in uMRD and pMRD patients was conducted on a subset of patients with available FCS files. Immune cell subsets and related metrics, such as granulocyte-to-lymphocyte ratio (GLR), were assessed to identify possible immune factors linked to MRD status. PCD and PCST tubes were analysed through FlowCT[12], a semi-automated computational workflow for the deconvolution of immunophenotypic data and the generation of objective reports from large-scale datasets. Automated clustering was performed using the FlowSOM and Seurat algorithms, and the resulting clusters were characterized and annotated with the Infinicyt software.

Results

Patient's characteristics

All patients evaluated for MRD from the date of adoption of the presented method (January 2022) until February 2025, were considered for this statistical analysis. Since the adoption of the method, 74 patients (median age 64 y, M/F: 38/36) (Table 1 and Supplementary table 1) with MM undergoing treatment, both transplant eligible (TE – we included in this group salvage ASCT at relapse) (n=58) and not transplant eligible (NTE) (n=16), have been evaluated by our center. Fifty-four out of 74 patients underwent an autologous stem cell transplantation (ASCT) and, as induction regimen, received Dara-VTD (n=35), Dara-VTD followed by Dara-RD (due to intolerance to thalidomide and bortezomib) (Dara-VTD/Dara-RD, included in the Dara-Rd group) (n=1), VTD (n=6), VCD (n=2), Isa-Kd (n=1), Dara-VRD (n=1), Kd (n=1), Dara-Vd (n=1), Dara-Rd (n=3) and KRD (n=3). Sixteen patients were not eligible for transplantation and were treated with Dara-Rd (n=8), Dara-Vd (n=2), VRD (n=1), VD (n=1), Teclistamab (n=2), Daratumumab monotherapy (n=1) and Belantamab (n=1). Four patients have been evaluated during maintenance with Lenalidomide. Concerning the Ig isotype, twenty-seven patients were typed as IgGκ, 19 IgGλ, 6 IgAκ , 4 IgAλ, 10 light chain κ and 6 light chain λ, and 2 of unknown isotype. Regarding the ISS stage, 17 patients were ISS I, 20 ISS II and 33 ISS III (unavailable ISS: 4 patients).

MRD single evaluation

We conducted 97 MRD evaluations using NGF-based protocol, achieving a median LOD of $1*10^{-5}$ and an average number of events per sample of $2.19*10^{6}$ (range: $2.0*10^{5}$– $6.98*10^{6}$). The maximum sensitivity recorded was $<3*10^{-6}$. A notable improvement in the number of acquired events over time was observed which led to a significant increase in the sensitivity of the test, likely due to refinements in sample preparation procedures (Supplementary Figure 1A). To assess the potential impact of delayed sample processing on marker stability, we compared samples processed within 24 hours of collection with those processed between 24 and 48 hours. No significant differences were observed in the MFI of any marker included in the EuroFlow PCD/PCST panels when evaluated on lymphocyte populations used as internal biological controls

(Supplementary Figure 1B-C), supporting the analytical robustness of the workflow within this timeframe. Among the assessed samples, twenty-one were post-induction therapy (22% of the total), twenty-eight were post-auto ASCT (29% of the total), seventeen (17% of the total) were during follow-up (>12 months after ASCT), eight (8% of the total) were in patients not eligible for ASCT, while 23 (24% of the total) were performed as a MRD confirmation or re-assessment. Of the 97 evaluations (Figure 1A and Supplementary Figure 1D), 47 resulted pMRD, 38 reached uMRD, and and 1 was not evaluable due to marked hemodilution and was therefore excluded from MRD assessment (considered as pMRD for outcome analyses). Notably, no samples were excluded because of clot formation. After a median follow-up period of 19 months, among 73 (out of 74) patients for whom outcome information were available, one progression event occurred in the uMRD group, while 15 pMRD cases experienced relapse and began subsequent treatment (three deaths were recorded in this group). Consequently, patients with uMRD had significantly longer PFS compared to those with pMRD (p=0.0056, Figure 1B). Among other variables, patients in the pMRD group showed a trend towards being more likely IgGκ (p=0.07), however, this finding should be interpreted with caution given the limited sample size and may reflect random variation rather than a true biological association. No associations were found with sex, ISS stage, treatment or ASCT eligibility. The latter finding could be related to the type of drug combination used or to the different time-points identified, taking into account that, in line with what reported in clinical trials, we observed a uMRD rate of 46% for Dara-VTD patients and 33% for Dara-RD.

MRD multiple evaluations

Eighteen patients underwent multiple evaluations. Of these, 11 patients were evaluated both at the end of induction and post-ASCT, 6 during the maintenance phase and 1 patient at 12 months after the first MRD evaluation during Dara-RD treatment. Four patients (all within maintenance treatment) received a third BM evaluation. Nine patients presented a sustained uMRD at 12 months, 3 patients a persistent pMRD and 6 patients showed a pMRD to uMRD conversion along the treatment. Interestingly, none of the patients that experienced a conversion from pMRD to uMRD progressed during the observation period.

Immune system assessment in pMRD and uMRD patients

Samples from 20 patients, for whom FCS samples were available at diagnosis and after treatment, were included in this exploratory analysis, encompassing both TE (17/20) and NTE (3/20) patients. Among these, 9 patients exhibited MRD persistence, while 11 were uMRD. After unsupervised clustering, BM populations were identified according to marker expression (Figure 3A-C and Supplementary figures 2-4); several changes were found after treatment in both uMRD and pMRD patients (+100 post-ASCT for TE patients, after VGPR for NTE patients). Overall, we observed a reduction of granulocytes (p=0.0012), in all T lymphocyte

populations and CD56^{dim} NK cells (p=0.0091, with a consequent increase of the CD56^{+}/CD56^{dim} NK ratio) and an increase of erythroblasts (p=0.000043) between baseline assessment and follow-up (Supplementary figure 5). Regarding the differences between patients with pMRD and uMRD, we noted that the latter exhibited a higher baseline BM granulocyte to lymphocytes ratio (BM GLR) compared to the former (p=0.038) (Figure 3D). Subsequent re-evaluations revealed an increased population of erythroblasts and B lymphocytes in uMRD patients (p=0.031 and p=0.045, respectively) coupled with a lower percentage of CD56^{dim} NK cells, compared to pMRD patients (p=0.014), which may reflect a more complete BM recovery after ASCT (Figure 3E). To assess whether these findings were influenced by the inclusion of the three NTE patients, we repeated all immune profiling analyses after restricting the cohort to transplant-eligible patients only. Overall, the main findings were preserved, with comparable immune remodeling after treatment and similar differences between uMRD and pMRD patients, although minor variations in statistical significance were observed because of the reduced sample size (Supplementary Figures 6 and 7). These findings suggest that immune profiling performed on the same datasets used for MRD assessment may provide additional information on the biological context associated with treatment response and depth of remission.

Conclusions

Our study reinforces the growing body of evidence supporting the feasibility and potential clinical relevance of MRD assessment via NGF in routine clinical practice for patients with MM. By utilizing two CE-IVD commercial EuroFlow tubes, we demonstrated the practical implementation of a standardized MRD detection strategy in a real-world clinical setting. This aspect is particularly relevant because, although NGF-based MRD assessment has been extensively validated in clinical trials, its integration into routine clinical workflows remains heterogeneous across laboratories[2]. Our findings therefore provide additional real-world evidence supporting the applicability and reproducibility of standardized NGF approaches in everyday clinical practice. In line with previous evidence from clinical trials, MRD negativity was associated with improved clinical outcomes in our real-world cohort. Prior studies have consistently shown that MRD negativity is associated with longer PFS and OS in MM, both in ASCT-eligible and ineligible patients. For instance, a study by Paiva et al. emphasized that achieving MRD negativity using NGF correlated with significantly better PFS and OS, highlighting the prognostic value of sensitive MRD detection methods[14]. Our results, showing a LOD of $1x10^{-5}$ and MRD undetectability in around 45% of the assessments, are consistent with these findings, reinforcing the robustness of NGF in real-world clinical settings. Moreover, our exploration of BM immune populations provides additional insights into the immunological landscape associated with MRD status. Notably, uMRD patients exhibited a higher bone marrow granulocyte-to-lymphocyte ratio compared to MRD-persistent patients. This observation parallels the findings by our group and other researchers on the role of BM granulocytes in achieving deep and prolonged response in MM[9,15]. For example, recent studies have shown that changes in immune cell subsets, such as NK cell activity and T-cell composition, may correlate with MRD negativity and improved clinical outcomes[11]. The integration of MRD assessment with bone marrow immune

profiling may provide a more comprehensive and biologically meaningful evaluation of treatment response, potentially improving patient stratification in future clinical settings. Importantly, the immune profiling component of our study was performed as an exploratory post-hoc analysis on a limited subset of patients with available FCS files. Therefore, the associations observed between BM immune composition, including the granulocyte-to-lymphocyte ratio, and MRD status should be interpreted as hypothesis-generating observations rather than definitive predictive biomarkers. Nevertheless, these findings suggest that integrating immune profiling into MRD assessment workflows may provide additional insights into the biological mechanisms underlying deep treatment responses. In terms of methodology, the integration of a semi-supervised bioinformatic algorithm in our study facilitated a detailed analysis of BM immune populations at a single-cell resolution. This innovative approach allowed us to create a comprehensive map of immune population distribution, which can be instrumental in understanding the immunological underpinnings of MRD dynamics. Other studies, such as the PETHEMA/GEM[16], have also employed advanced computational tools to analyze MRD and immune responses, demonstrating the increasing relevance of bioinformatics in enhancing the precision of MRD assessments. Comparing our findings with those utilizing NGS for MRD detection, we observe that both NGF and NGS have their unique advantages and limitations. While NGS offers high sensitivity and patient-specific molecular marker detection, NGF provides rapid turnaround times and comprehensive immune profiling capabilities that could be of utmost importance in a routine clinical practice setting. Studies by Martínez-López and others, have highlighted the complementary nature of these methods, suggesting that a combined approach might offer the most comprehensive assessment of MRD and its clinical implications[17]. In conclusion, our study supports the feasibility and suggests the potential clinical relevance of MRD assessment via NGF in real-world, offering valuable insights into the prognostic and immunological aspects of MM. These findings may be particularly relevant in light of the results of a recent phase 3 clinical trial investigating the use of quadruplets in first-line settings[18–20]. Specifically, the Perseus trial has examined the possibility of discontinuing Daratumumab after 24 months from CR achievement once uMRD has been maintained for at least 12 months[18]. In this context, the availability of standardized and reproducible methods for MRD detection, such as the approach evaluated in this study, may facilitate the translation of clinical trial results into clinical practice. The consistency of our findings with previous clinical studies further supports the robustness of NGF performed using the PCD/PCST diagnostic tool as a reliable and feasible approach for MRD assessment in routine clinical practice. These results reinforce the potential value of standardized flow-based MRD monitoring and support its integration into clinical workflows, including future (and current) MRD-driven treatment strategies such as therapy de-escalation in patients achieving sustained uMRD[18]. An additional practical aspect supporting the implementation of NGF in routine clinical practice is the reproducibility of marker detection despite unavoidable variations in sample processing times. In our cohort, lymphocyte populations were used as internal biological controls, and no significant differences in marker MFI were observed between samples

processed within 24 hours and those processed between 24 and 48 hours after collection. These findings further support the robustness of the standardized workflow under real-world conditions.

Our study has several limitations that should be acknowledged. First, this was a single-center study with both prospective and retrospective components, which may have introduced selection and reporting biases and may limit the generalizability of the findings. Second, although the overall number of MRD assessments was sufficient to demonstrate the feasibility of the approach, the relatively small sample size limited the statistical power of the study, particularly for subgroup analyses and longitudinal MRD evaluations. As a result, robust comparisons across different treatment strategies and a comprehensive assessment of sustained MRD negativity over time were not feasible. Moreover, MRD assessments were performed at different clinically relevant timepoints, including post-induction, post-ASCT, and during follow-up, reflecting real-world practice but introducing additional heterogeneity in the interpretation of MRD status. Similarly, the cohort size remained limited for more granular analyses based on immune profiling. We observed a trend toward an association between IgG isotype and MRD persistence; however, this finding did not reach statistical significance and should therefore be interpreted with caution. Given the limited sample size and the clinical heterogeneity of the population, this observation should be considered hypothesis-generating and requires validation in independent cohorts. Third, while the duration of follow-up was adequate to capture early relapse events, it may be insufficient to fully evaluate long-term clinical outcomes, particularly overall survival. Furthermore, the limited number of progression events observed among uMRD patients precludes definitive conclusions regarding the durability of responses in this subgroup. Finally, although the application of semi-automated computational tools enabled an in-depth characterization of the bone marrow immune microenvironment, the exploratory nature of these immunophenotypic analyses limits their immediate generalizability.

Prospective multicenter studies with larger cohorts, longer follow-up, and comprehensive clinical annotation are needed to further define the prognostic and therapeutic implications of MRD assessment in multiple myeloma. Future investigations should also evaluate the integration of immune profiling and advanced computational approaches with established MRD methodologies, as well as the complementary use of NGF and NGS, to further improve the precision and clinical utility of MRD-guided patient management.

References

1. Gullà A, Dhodapkar MV, Einsele H, et al. Rethinking multiple myeloma treatment: the biological and clinical insights guiding immune-based combinations. Blood Cancer Discov. 2026;7(2):176-194.

2. Mina R, Antonioli E, Barilà G, et al. Undetectable minimal residual disease in multiple myeloma: bridging the gap between clinical trials and real-life application. Clin Lymphoma Myeloma Leuk. 2025;26(3):154-168.

3. Landgren O, Prior TJ, Masterson T, et al. EVIDENCE meta-analysis: evaluating minimal residual disease as an intermediate clinical end point for multiple myeloma. Blood. 2024;144(4):359-367.

4. Lahuerta JJ, San-Miguel J, Jiménez-Ubieto A, et al. High-dose busulfan-melphalan vs melphalan and reinforced VRD for newly diagnosed multiple myeloma: a phase 3 GEM trial. Blood. 2025;146(15):1747-1758.

5. Shi Q, Paiva B, Pederson LD, et al. Minimal residual disease-based end point for accelerated assessment of clinical trials in multiple myeloma: a pooled analysis of individual patient data from multiple randomized trials. J Clin Oncol. 2025;43(11):1289-1301.

6. Kumar S, Paiva B, Anderson KC, et al. International Myeloma Working Group consensus criteria for response and minimal residual disease assessment in multiple myeloma. Lancet Oncol. 2016;17(8):e328-e346.

7. Flores-Montero J, Sanoja-Flores L, Paiva B, et al. Next generation flow for highly sensitive and standardized detection of minimal residual disease in multiple myeloma. Leukemia. 2017;31(10):2094-2103.

8. Walzer S, Krenberger S, Vollmer L, Hewitt T, Eckert B. A Cost Impact Analysis of clonoSEQ® as a valid and CE-certified minimal residual disease (MRD) diagnostic compared to no MRD testing in multiple myeloma in Germany. Oncol Ther. 2021;9(2):607-619.

9. Guerrero C, Puig N, Cedena M-T, et al. A machine learning model based on tumor and immune biomarkers to predict undetectable MRD and survival outcomes in multiple myeloma. Clin Cancer Res. 2022;28(12):2598-2609.

10. Firestone RS, Simhal AK, McAvoy D, et al. Immune MRD status informs tumor MRD outcome prognostication in patients with multiple myeloma on lenalidomide maintenance. Clin Cancer Res. 2025;31(21):4446-4456.

11. Korst CLBM, Tahri S, Duetz C, et al. The bone marrow NK-cell profile predicts MRD negativity in patients with multiple myeloma treated with daratumumab-based therapy. Blood. 2025;145(25):3007-3014.

12. Botta C, Maia C, Garcés J-J, et al. FlowCT for the analysis of large immunophenotypic data sets and biomarker discovery in cancer immunology. Blood Adv. 2022;6(2):690-703.

13. Puig N, Flores-Montero J, Burgos L, et al. Reference values to assess hemodilution and warn of potential false-negative minimal residual disease results in myeloma. Cancers (Basel). 2021;13(19):4924.

14. Paiva B, Shi Q, Puig N, et al. Opportunities and challenges for MRD assessment in the clinical management of multiple myeloma. Nat Rev Clin Oncol. 2025;22(6):424-438.

15. Corsale AM, Azgomi MS, Gigliotta E, et al. Bone marrow immune cell composition reflects multiple myeloma progression and affects treatment response. Blood Neoplasia. 2026;3(1):100174.

16. Arana P, Paiva B, Cedena M-T, et al. Prognostic value of antigen expression in multiple myeloma: a PETHEMA/GEM study on 1265 patients enrolled in four consecutive clinical trials. Leukemia. 2018;32(4):971-978.

17. Martinez-Lopez J, Lahuerta JJ, Pepin F, et al. Prognostic value of deep sequencing method for minimal residual disease detection in multiple myeloma. Blood. 2014;123(20):3073-3079.

18. Sonneveld P, Dimopoulos MA, Boccadoro M, et al. Daratumumab, bortezomib, lenalidomide, and dexamethasone for multiple myeloma. N Engl J Med. 2024;390(4):301-313.

19. Usmani SZ, Facon T, Hungria V, et al. Daratumumab plus bortezomib, lenalidomide and dexamethasone for transplant-ineligible or transplant-deferred newly diagnosed multiple myeloma: the randomized phase 3 CEPHEUS trial. Nat Med. 2025;31(4):1195-1202.

20. Facon T, Dimopoulos M-A, Leleu XP, et al. Isatuximab, bortezomib, lenalidomide, and dexamethasone for multiple myeloma. N Engl J Med. 2024;391(17):1597-1609.

Table 1. Patients' characteristics

PATIENTS' CHARACTERISTICS		N = 74
AGE		64 (36 -78)
SEX		
	F	36 (49%)
	M	38 (51%)
ISS		
	I	17 (23%)
	II	20 (27%)
	III	33 (45%)
	N/A	4 (5%)
ISOTYPE		
	IgA/κ	6 (8%)
	IgA/λ	4 (5%)
	IgG/κ	27 (36%)
	IgG/λ	19 (26%)
	κ	10 (14%)
	λ	6 (8%)
	N/A	2 (3%)
MRD STATUS		
	uMRD	32 (43%)
	pMRD	41 (56%)
	NE	1 (1%)

Figure 1. NGF-based measurable residual disease (MRD) status is associated with treatment response and improved progression-free survival in patients with multiple myeloma (A) *Treatment lines and MRD dynamics*. Entire cohort (N = 73), stratified from initial treatment eligibility classification (TE/NTE) through specific treatment regimens to MRD assessment and disease progression status. The majority of patients received transplant-eligible (TE) therapy (78.1%, n = 57), with Daratumumab-VTD being the most common treatment regimen (46.6%, n = 34). After the treatment, 43.8% (n=32) achieved uMRD status, which was associated with significantly lower rates of disease progression. Overall, 79.5% (n=58) of patients remained progression-free during the follow-up period. (B) *Progression-free survival by MRD status.* The uMRD group (red line, 45%, N=32) had significantly longer PFS than pMRD patients (blue line, n= 41; log-rank *p<0.001). One relapse occurred in uMRD vs. 15 in pMRD (including 3 progression-related deaths) after a median follow-up of 19 months. The survival analysis demonstrates a statistically significant PFS advantage in uMRD patients (p<0.001), reinforcing the prognostic power of NGF-based MRD negativity as a surrogate marker for long-term disease control in MM.

Figure 2. Longitudinal MRD monitoring demonstrates a more favorable clinical course in patients with baseline uMRD than in those with baseline pMRD. Swimmer plot of patients with pMRD (left) or uMRD (right) at baseline. Each horizontal bar represents the follow-up duration from the first MRD assessment. Circles indicate subsequent MRD evaluations (green = uMRD; red = pMRD). Bar color reflects clinical outcome: green for patients without relapse, red for those who experienced relapse. Patients were evaluated at various treatment phases, including post-induction, post-autologous stem cell transplant (ASCT), and during maintenance. Sequential assessments highlight dynamic MRD changes and their association with relapse risk.

Figure.3 Immune profiling identifies distinct immune cell compositions associated with MRD status in multiple myeloma (A) Uniform manifold approximation and projection (UMAP) of eosinophils ($CD45^{+bright}$, SCC^{high}), erythroblasts ($CD45^{-}$, $CD38^{-}$, SCC^{low}), granulocytes ($CD45^{+dim}$, SCC^{high}), lymphocytes ($CD45^{+}$, SCC^{low}), monocytes ($CD45^{+}$, SCC^{int}) and plasma cells ($CD138^{+}$, $CD38^{+high}$) identified by self-organizing map (SOM). (B) Lymphocyte subsets were subclustered based on the median expression of individual markers within each cell cluster in BD OneFlow™ PCD tube. (C) Lymphocyte subsets were subclustered based on the median expression of individual markers within each cell cluster in BD OneFlow™ PCST tube. (D) Box plot depicting the frequency of granulocytes and the ratio of granulocyte to lymphocyte frequencies at baseline between pMRD and uMRD MM patients. (E) Box plot representing the frequency of erythroblasts, B lymphocytes, and $CD56^{dim}$ NK cells at follow-up between pMRD and uMRD MM patients.

Figure 1

A

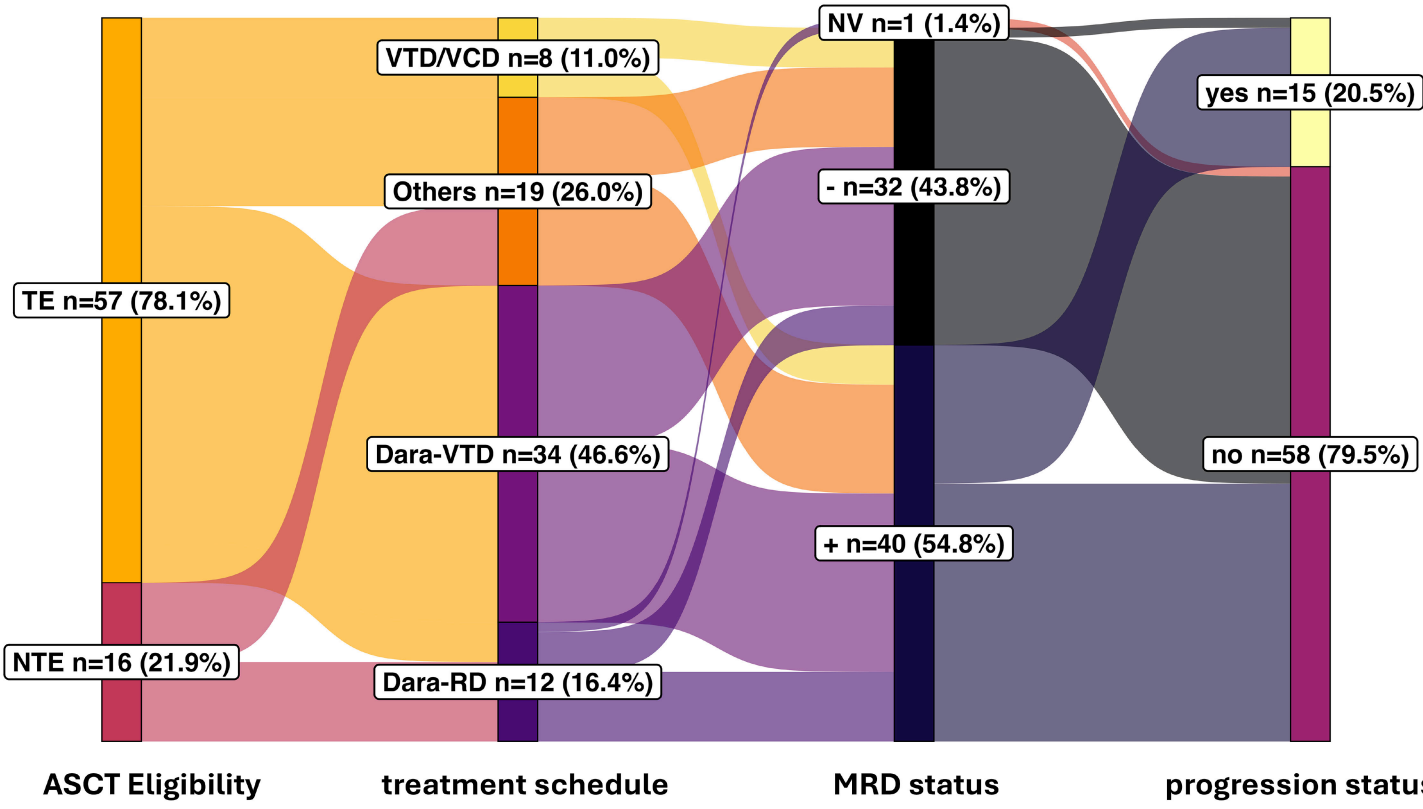
TE n=57 (78.1%)
NTE n=16 (21.9%)
VTD/VCD n=8 (11.0%)
Others n=19 (26.0%)
Dara-VTD n=34 (46.6%)
Dara-RD n=12 (16.4%)
NV n=1 (1.4%)
- n=32 (43.8%)
+ n=40 (54.8%)
yes n=15 (20.5%)
no n=58 (79.5%)
ASCT Eligibility
treatment schedule
MRD status
progression status

B

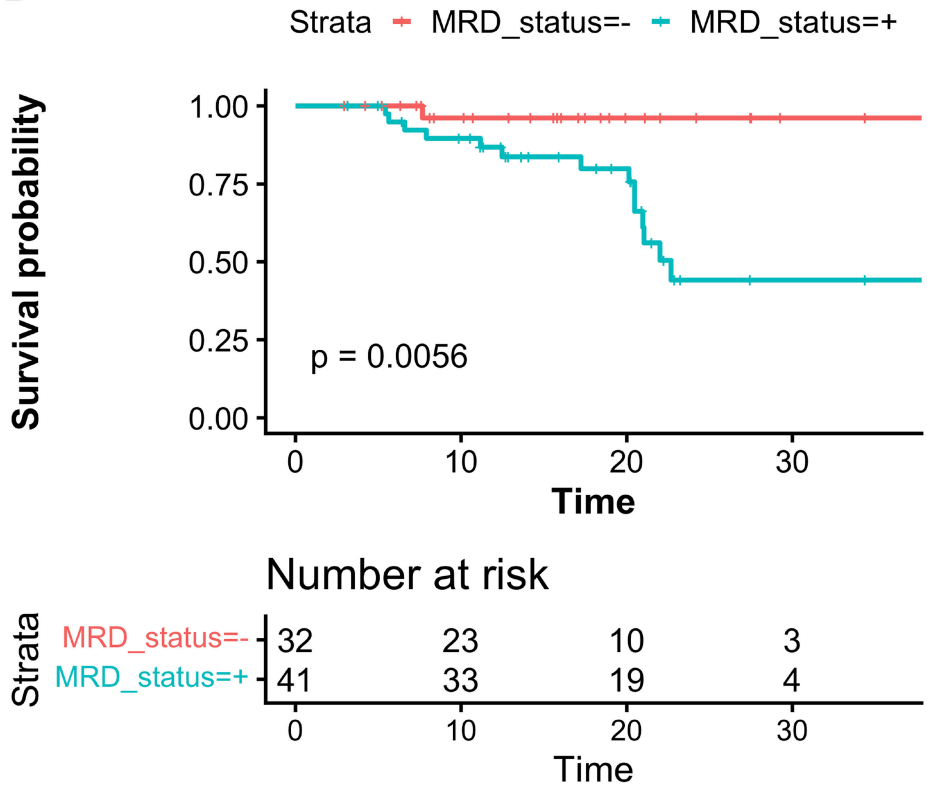
Strata MRD_status=- MRD_status=+
Survival probability
1.00
0.75
0.50
0.25
0.00
p = 0.0056
0
10
20
30
Time
Number at risk
Strata
MRD_status=- 32 23 10 3
MRD_status=+ 41 33 19 4
0
10
20
30
Time

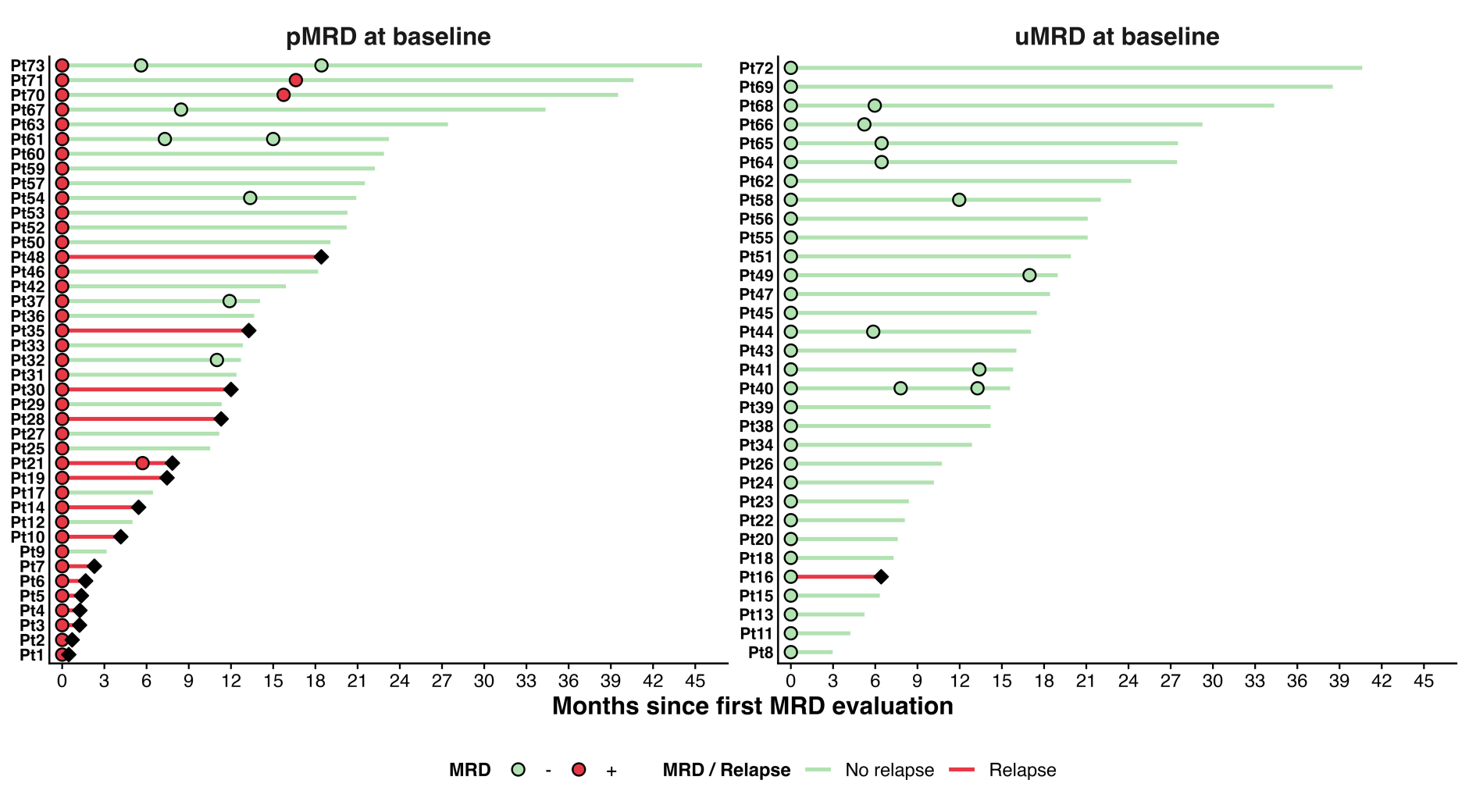
pMRD at baseline
uMRD at baseline
Pt73
Pt71
Pt70
Pt67
Pt63
Pt61
Pt60
Pt59
Pt57
Pt54
Pt53
Pt52
Pt50
Pt48
Pt46
Pt42
Pt37
Pt36
Pt35
Pt33
Pt32
Pt31
Pt30
Pt29
Pt28
Pt27
Pt25
Pt21
Pt19
Pt17
Pt14
Pt12
Pt10
Pt9
Pt7
Pt6
Pt5
Pt4
Pt3
Pt2
Pt1
Pt72
Pt69
Pt68
Pt66
Pt65
Pt64
Pt62
Pt58
Pt56
Pt55
Pt51
Pt49
Pt47
Pt45
Pt44
Pt43
Pt41
Pt40
Pt39
Pt38
Pt34
Pt26
Pt24
Pt23
Pt22
Pt20
Pt18
Pt16
Pt15
Pt13
Pt11
Pt8
0 3 6 9 12 15 18 21 24 27 30 33 36 39 42 45
Months since first MRD evaluation
MRD - +
MRD / Relapse
No relapse
Relapse

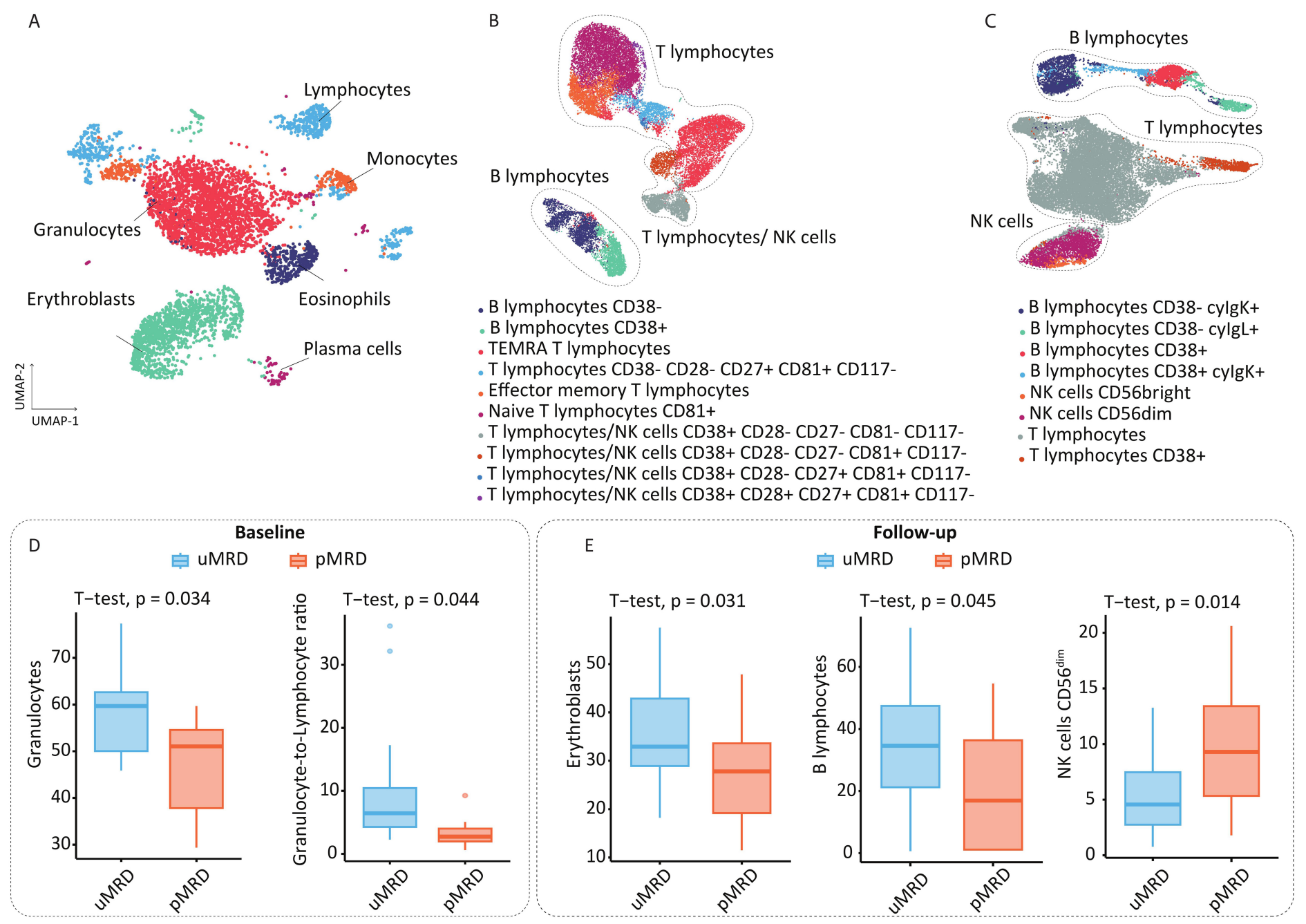
A
Lymphocytes
Monocytes
Granulocytes
Erythroblasts
Eosinophils
Plasma cells
UMAP-2
UMAP-1
B
T lymphocytes
B lymphocytes
T lymphocytes/ NK cells
B lymphocytes CD38-
B lymphocytes CD38+
TEMRA T lymphocytes
T lymphocytes CD38- CD28- CD27+ CD81+ CD117-
Effector memory T lymphocytes
Naive T lymphocytes CD81+
T lymphocytes/NK cells CD38+ CD28- CD27- CD81- CD117-
T lymphocytes/NK cells CD38+ CD28- CD27- CD81+ CD117-
T lymphocytes/NK cells CD38+ CD28- CD27+ CD81+ CD117-
T lymphocytes/NK cells CD38+ CD28+ CD27+ CD81+ CD117-
C
B lymphocytes
T lymphocytes
NK cells
B lymphocytes CD38- cyIgK+
B lymphocytes CD38- cyIgL+
B lymphocytes CD38+
B lymphocytes CD38+ cyIgK+
NK cells CD56bright
NK cells CD56dim
T lymphocytes
T lymphocytes CD38+
D
Baseline
uMRD
pMRD
T−test, p = 0.034
Granulocytes
T−test, p = 0.044
Granulocyte-to-Lymphocyte ratio
E
Follow-up
uMRD
pMRD
T−test, p = 0.031
Erythroblasts
T−test, p = 0.045
B lymphocytes
T−test, p = 0.014
NK cells CD56dim

Supplementary data

Supplementary table 1

MRD	Total = 97
Events (average/min-max)	2.16×10^6 (2.35×10^5 – 6.99×10^6)
LOD (average/min-max)	0.0007 (0.0003 - 0.028); 7×10^{-6}

Treatment	Total = 74
Dara-VTd	35
Dara-VTd/Dara-Rd	1
VTd	6
VCd	2
Isa-Kd	1
Dara-VRd	1
Kd	1
Dara-Vd	3
Dara-Rd	11
KRd	3
Belantamab	1
Daratumumab (monotherapy)	1
VRd	1
Vd	1
Lenalidomide maintenance	4
Teclistamab	2

Supplementary Figure 1

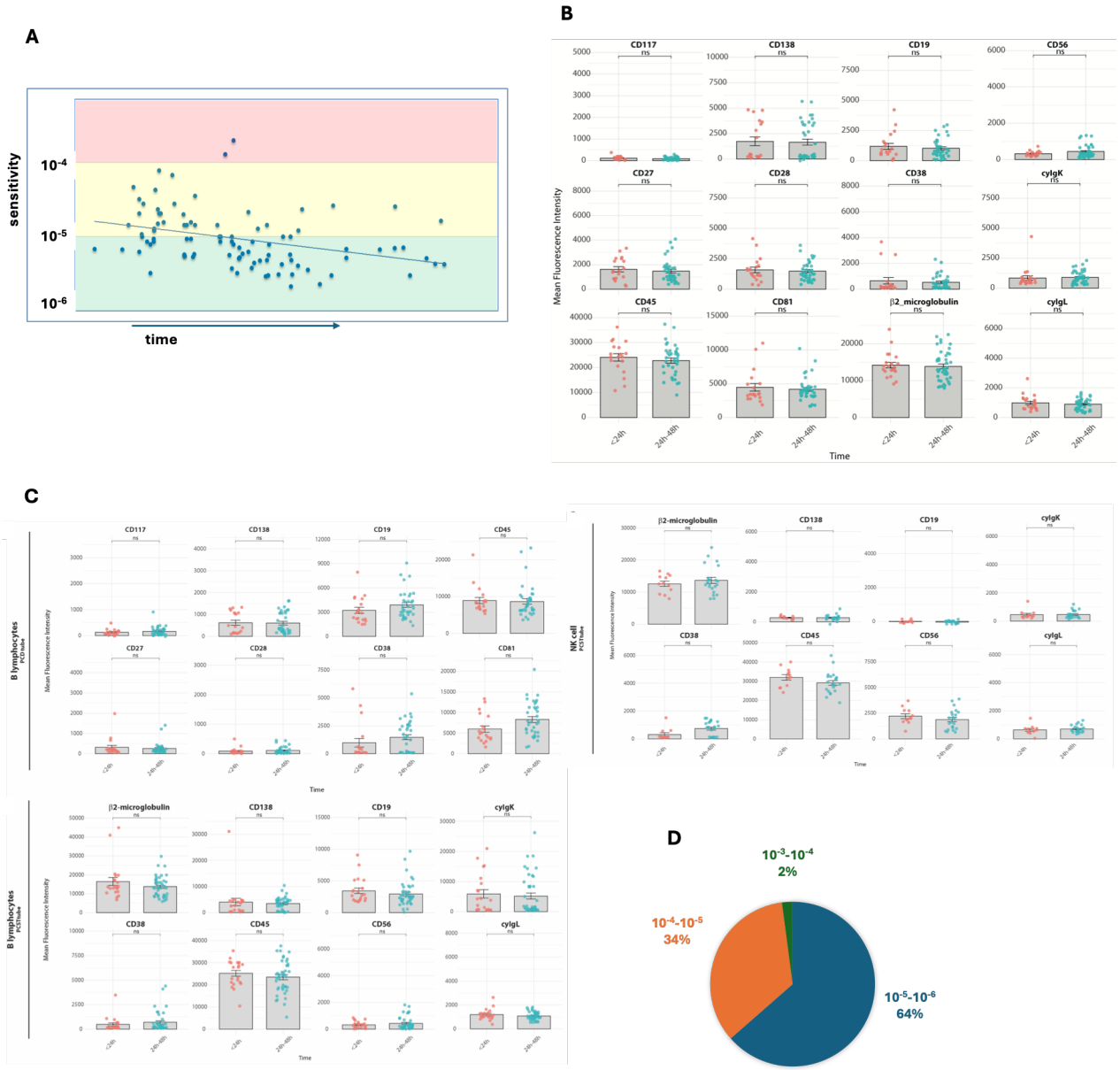

Supplementary figure 1

(A) Distribution of assay sensitivity over time. Each dot represents an individual sample; shaded areas indicate sensitivity ranges (10^{-3}–10^{-4}, 10^{-4}–10^{-5}, and 10^{-5}–10^{-6}). The line depicts the overall temporal trend. (B) MFI of markers included in the PCD tube (CD117, CD138, CD19, CD27, CD28, CD38, CD45, and CD81) and in the PCST tube (β2-microglobulin, CD138, CD19, CD38, CD45, CD56, cytoplasmic Igκ, and cytoplasmic Igλ) expressed on whole lymphocyte population measured in bone marrow samples processed within 24 hours (<24 h) or between 24 and 48 hours (24–48 h) after collection. Data are shown as box-and-whisker plots with individual samples overlaid. (C) MFI of markers included in the PCD and in the PCST tube expressed on B lymphocytes and NK cells measured in bone marrow samples processed within 24 hours (<24 h) or between 24 and 48 hours (24–48 h) after collection. Data are shown as box-and-whisker plots with individual samples overlaid. (D) Pie chart showing the distribution of assay sensitivity across the 97 analyzed samples. Abbreviations: MFI, Mean fluorescence intensity; PCD, Plasma Cell Disorder; PCST, Plasma Cell Screening Tube.

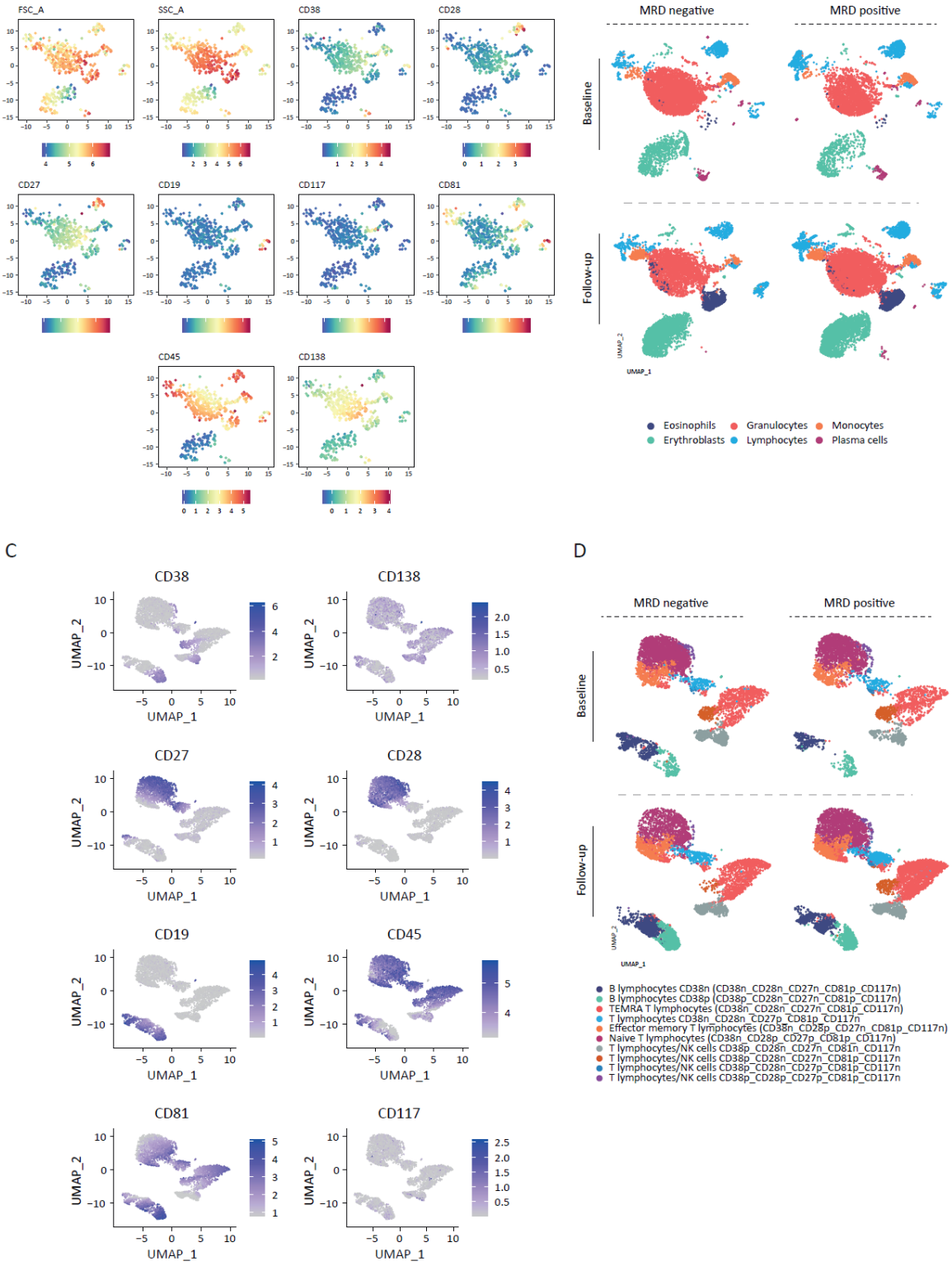

Supplementary figure 2. FlowCT analysis of BD OneFlow™ PCD tube.

(A) Uniform manifold approximation and projection (UMAP) of identified by self-organizing map (SOM) of BD OneFlow™ PCD tube. (B) Uniform manifold approximation and projection (UMAP) of main bone marrow immune cell populations at baseline and after follow-up in MRD negative and positive MM patients. (C) Feature plots depict the expression of each marker in a reduced-dimensional space after subclustering of lymphocyte populations. (D) Uniform manifold approximation and projection (UMAP) of lymphocyte populations at baseline and after follow-up in MRD negative and positive MM patients.

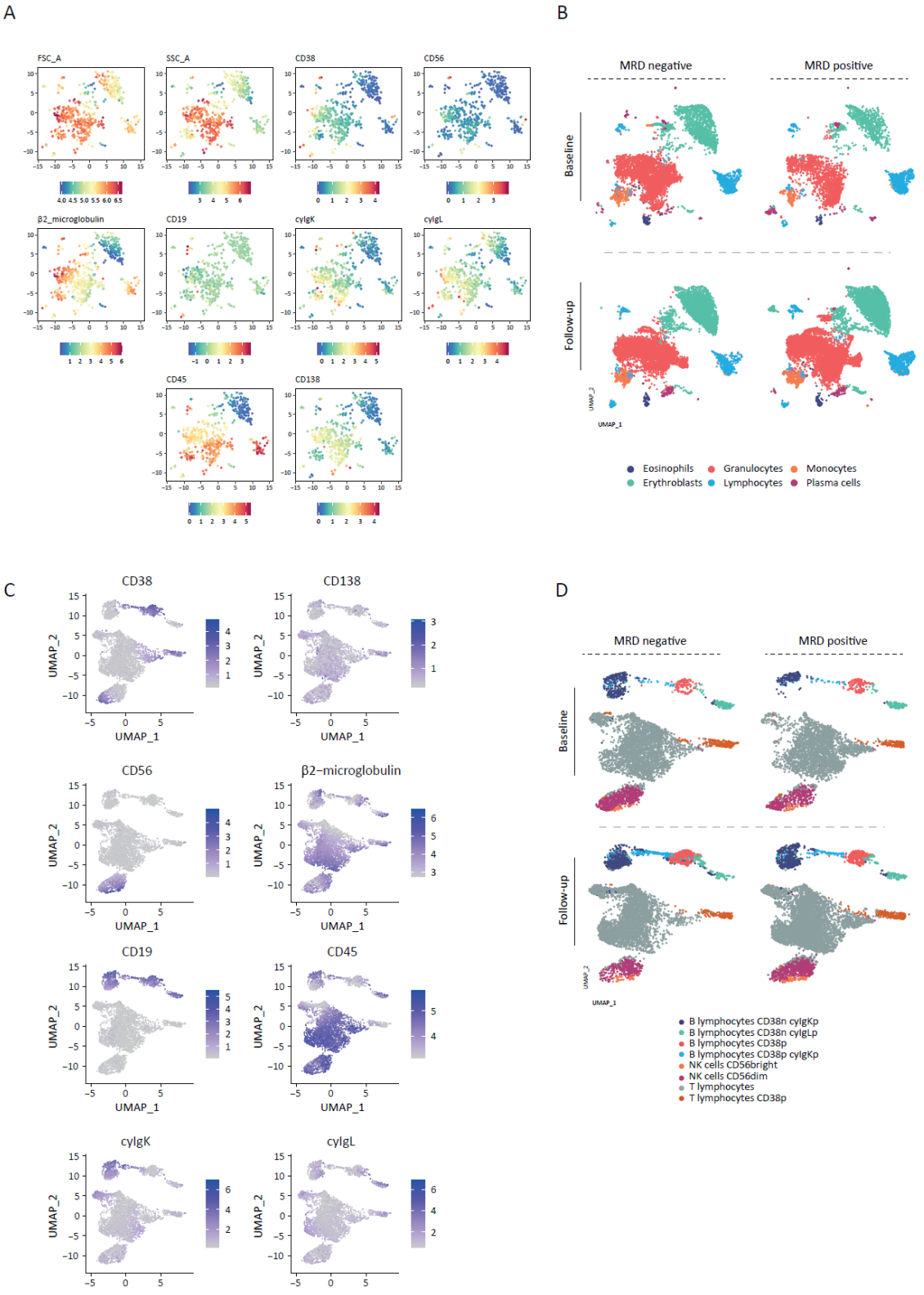

Supplementary figure 3. FlowCT analysis of BD OneFlow™ PCST tube.

(A) Uniform manifold approximation and projection (UMAP) of identified by self-organizing map (SOM) of BD OneFlow™ PCST tube. (B) Uniform manifold approximation and projection (UMAP) of main bone marrow immune cell populations at baseline and after follow-up in MRD negative and positive MM patients. (C) Feature plots depict the expression of each marker in a reduced-dimensional space after subclustering of lymphocyte populations. (D) Uniform manifold approximation and projection (UMAP) of lymphocyte populations at baseline and after follow-up in MRD negative and positive MM patients.

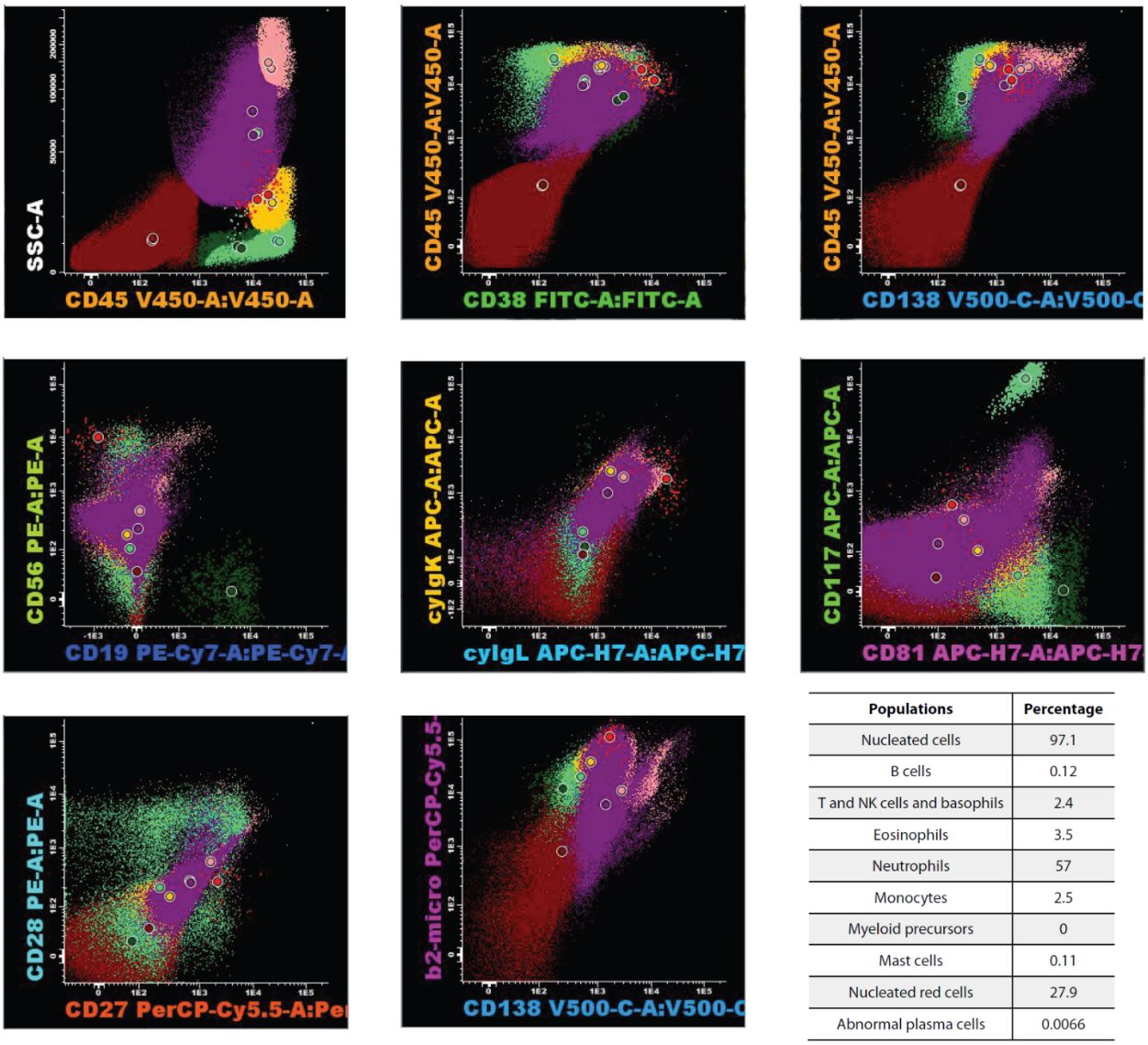

Populations	Percentage
Nucleated cells	97.1
B cells	0.12
T and NK cells and basophils	2.4
Eosinophils	3.5
Neutrophils	57
Monocytes	2.5
Myeloid precursors	0
Mast cells	0.11
Nucleated red cells	27.9
Abnormal plasma cells	0.0066

Supplementary figure 4. Gating strategy and distribution of cellular populations.

The figure illustrates the flow cytometry gating strategy used to identify the main cellular populations within the samples and their relative percentages.

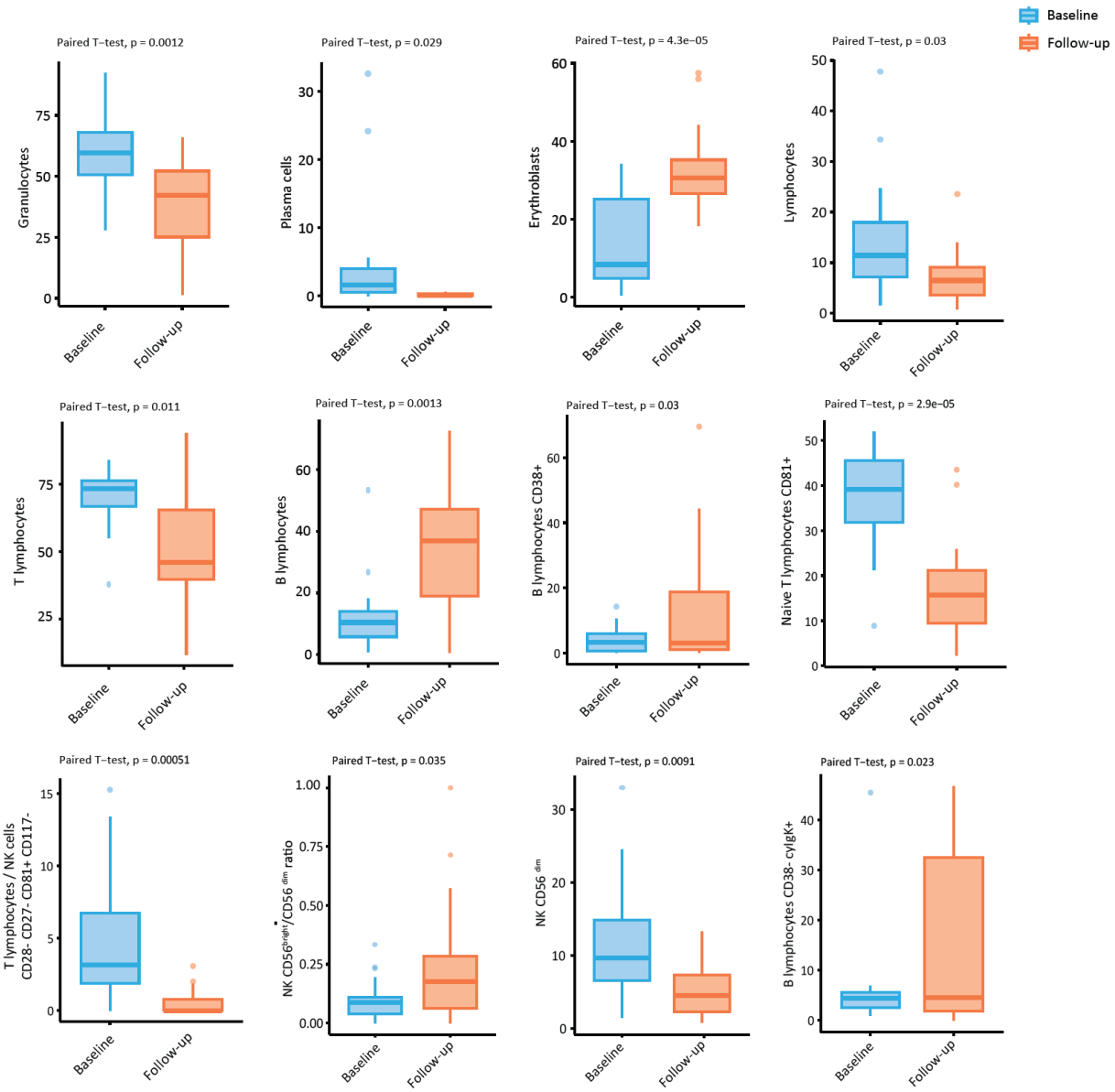

Supplementary figure 5. Longitudinal comparisons along treatments

Box plots showing the differential distribution of immune cell subsets at baseline and follow-up.

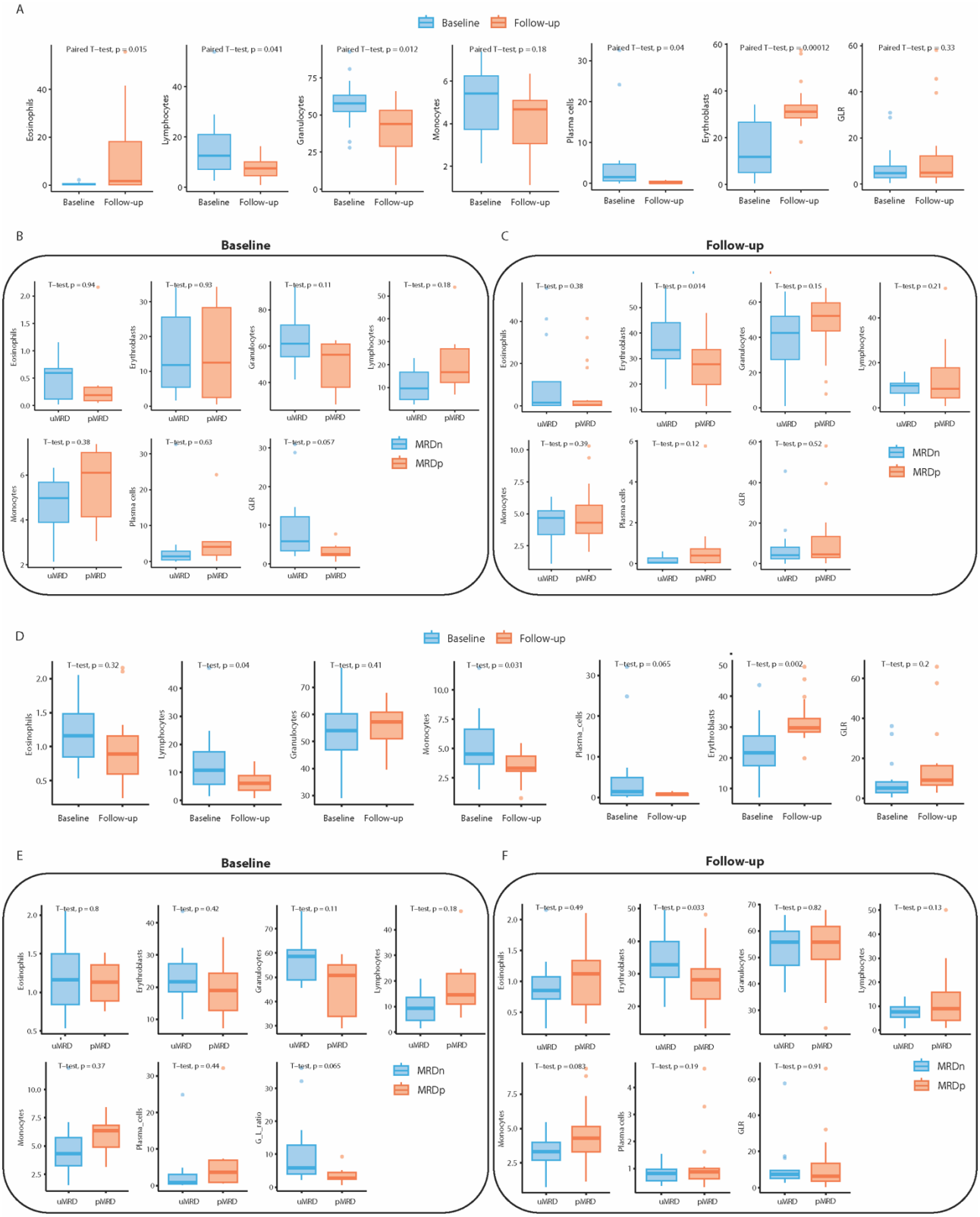

Supplementary figure 6. Longitudinal changes in major bone marrow cell populations and association with MRD status in transplant-eligible patients.

Box plots showing: (A) Paired comparison of eosinophils, lymphocytes, granulocytes, monocytes, plasma cells, erythroblasts, and GLR identified in PCD tube between baseline and follow-up bone marrow samples from TE-MM patients. (B–C) Comparison of the same cell populations according to MRD status (uMRD versus pMRD) at baseline (B) and follow-up (C) in PCD tube. (D) Paired comparison of eosinophils, lymphocytes, granulocytes, monocytes, plasma cells, erythroblasts, and GLR identified in PCST tube between baseline and follow-up bone marrow samples from TE-MM patients. (E–F) Comparison of the same cell populations according to MRD status (uMRD versus pMRD) at baseline (E) and follow-up (F) in PCST tube. Abbreviations: GLR, granulocyte-to-lymphocyte ratio; PCD, Plasma Cell Disorder; TE, transplant-eligible; uMRD, undetectable MRD; pMRD, persistent MRD; PCST, Plasma Cell Screening Tube.

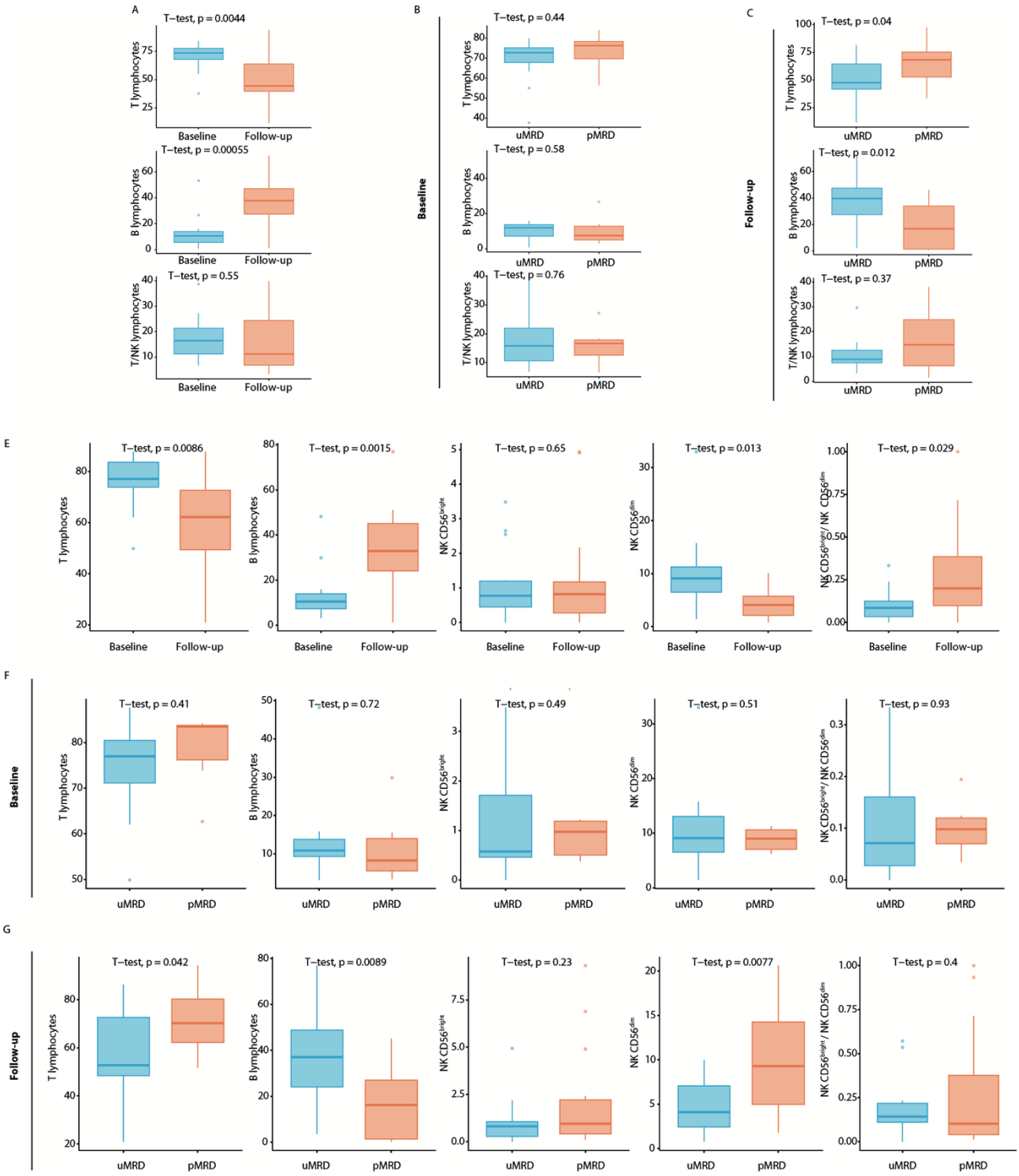

Supplementary figure 7. Longitudinal changes in lymphoid and NK-cell populations according to MRD status in transplant-eligible patients.

Box plots showing: ((A) Longitudinal changes in the frequencies of T lymphocytes, B lymphocytes, and T/NK lymphocytes identified in PCD tube between baseline and follow-up samples from TE-MM patients. (B–C) Comparison of lymphoid populations identified in PCD tube according to MRD status (uMRD versus pMRD) of TE-MM patients at baseline (B) and follow-up (C). (E) Longitudinal analysis of T lymphocytes, B lymphocytes, NK CD56bright cells, NK CD56dim cells, and the NK CD56bright/CD56dim ratio) identified in PCST between baseline and follow-up samples from TE-MM patients. (F–G) Comparison of lymphocyte and NK-cell subsets identified in PCST tube according to MRD status (uMRD versus pMRD) of TE-MM patients at baseline (F) and follow-up (G). Abbreviations: PCD, Plasma Cell Disorder; TE, transplant-eligible; uMRD, undetectable MRD; pMRD, persistent MRD; PCST, Plasma Cell Screening Tube.